Available online at www.sciencedirect.com

ScienceDirect

Mendeleev Commun., 2023, **33**, 160–163

Mendeleev Communications

Features of doxorubicin adsorption on Fe_3O_4 magnetic nanoparticles coated with SiO_2 or SiO_2/aminopropylsilane

Alexander M. Demin,*[a] Alexander V. Vakhrushev,[a] Marina S. Valova,[a] Marina A. Korolyova,[a] Mikhail A. Uimin,[b] Artem S. Minin,[b] Konstantin A. Chistyakov,[a] Victor P. Krasnov[a] and Valery N. Charushin[a]

[a] *I. Ya. Postovsky Institute of Organic Synthesis, Ural Branch of the Russian Academy of Sciences, 620108 Ekaterinburg, Russian Federation. Fax: +7 343 369 3058; e-mail: demin@ios.uran.ru*

[b] *M. N. Mikheev Institute of Metal Physics, Ural Branch of the Russian Academy of Sciences, 620990 Ekaterinburg, Russian Federation*

DOI: 10.1016/j.mencom.2023.02.004

New nanocomposites based on Fe_3O_4 magnetic nanoparticles coated with SiO_2 or SiO_2/aminopropylsilane (APS), including those using *N*-(phosphonomethyl)iminodiacetic acid (PMIDA), were obtained, and the immobilization of the antitumor agent doxorubicin (Dox) on nanocomposites was examined. It has been shown that the binding of Dox to the negatively charged surface of SiO_2 particles occurs more efficiently than that to the APS-modified surface with positively charged amino groups; the presence of PMIDA molecules on the surface significantly increased the loading content. Based on DFT calculations, a mechanism for Dox binding to the surface of the synthesized nanocomposites was proposed.

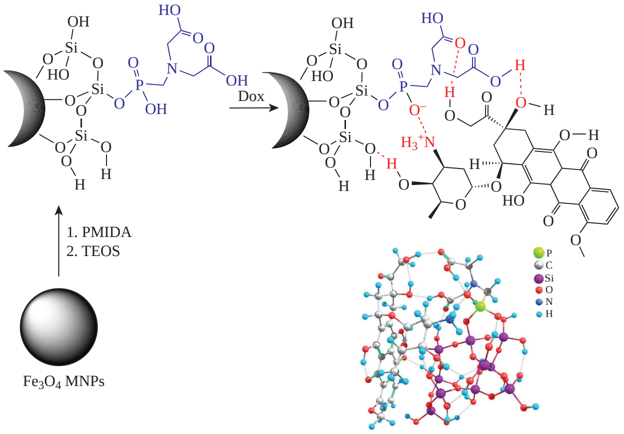

Keywords: nanocomposites, magnetic nanoparticles, surface functionalization, PMIDA, silica coating, doxorubicin, DFT.

Dedicated to Academician of the Russian Academy of Sciences Irina Petrovna Beletskaya on the occasion of her anniversary.

Currently, magnetic nanoparticles (MNPs) are widely used in the design of contrast agents for MRI and drug delivery systems, as well as in the synthesis of materials for biological applications.[1–6] Both natural and synthetic polymers, as well as silica, are used as coatings for MNPs. Silica is able to protect the core from destruction under physiological conditions,[7] increase the efficiency of particle functionalization by other molecules[8] or enhance the sorption capacity with respect to some drugs.[9] In the literature, there are examples of Dox sorption on SiO_2-based nanomaterials[10,11] or MNPs–SiO_2[5,12,13] with both a negatively charged surface and a positively charged surface modified with aminopropylsilane (APS).[13–15]

The purpose of our study is to compare the efficiency of immobilization of the anticancer agent doxorubicin (Dox) on SiO_2- and SiO_2/APS-coated nanocomposite materials depending on the nature of the surface, as well as to perform quantum chemical calculations of the mechanism of its binding.

The initial MNPs were synthesized by the coprecipitation method similarly to the described procedures.[3,8] Colloidal solutions of bare and stabilized Fe_3O_4 MNPs **1** were used for coating. Nanoparticles **1** in solution were stabilized with *N*-(phosphonomethyl)iminodiacetic acid (PMIDA) to obtain MNPs–PMIDA **2**. In this case, in contrast to the previously described methods,[3,8] the excess of the reagent was not removed from the reaction mixture. After that, a SiO_2 coating was applied using a 1.5 molar excess of TEOS (Scheme 1) to afford MNPs–SiO_2-1 **3** and MNPs–SiO_2-2 **4**. It is known that alkoxysilane reagents are fixed on the surface of Fe_3O_4 MNPs due to the formation of Fe–O–Si covalent bonds with the surface Fe–OH groups. Then nanocomposites **3** and **4** were modified with APS, as a result of which MNPs–SiO_2–APS-1 **5** and MNPs–SiO_2–APS-2 **6** were obtained, respectively.[†]

Nanocomposites MNPs–SiO_2-1 and MNPs–SiO_2-2 differ in their structure. Thus, the use of PMIDA leads to the formation of nanocomposites with a core of several MNPs surrounded by a thick SiO_2 shell. According to TEM data, the average core size of the synthesized nanocomposites is 9 nm. The sizes of MNPs–SiO_2-1 are 11–14 nm with a shell thickness of 2–3 nm, while the sizes of MNPs–SiO_2-2 are 26–50 nm with a shell thickness of 3.5–5.5 nm [Figure 1(*a*),(*b*)]. In the FTIR spectra (Figure 2) of these products, we observed the appearance of intense absorption bands in the region of 1070 cm^{-1}, which are related to vibrations of the Si–O bonds. The bands corresponding to the Fe–O vibrations in the modified products are shifted by ~15 cm^{-1} relative to the bands of the initial MNPs, which confirms the formation of a coating on the surface of the MNPs.

The content of organic components was determined by energy-dispersive X-ray spectroscopy (EDX) and CHN elemental analysis (Table 1). The EDX data confirm the higher content of SiO_2 in the corresponding nanocomposites obtained using PMIDA (see Table 1). Figure 3(*a*) shows the EDX spectrum of MNPs–SiO_2-2 as an example. It was also shown that up to 27% of the amount of

---

[†] For procedures, characterization of the nanomaterials obtained and computational details, see Online Supplementary Materials.

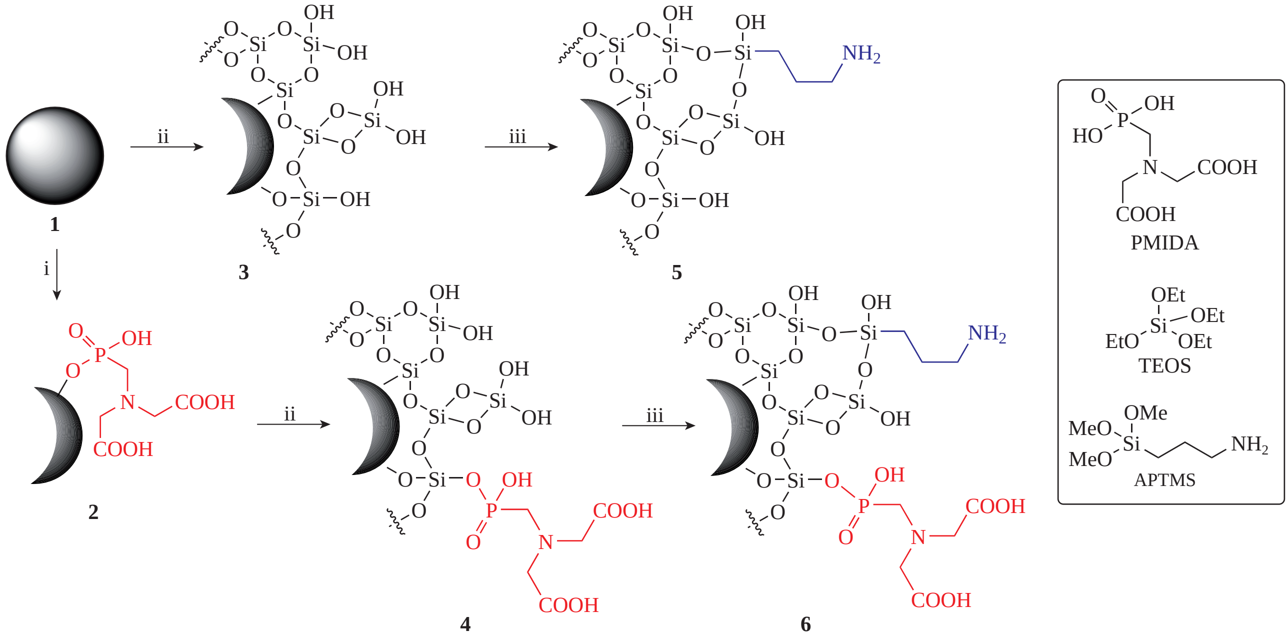

Scheme 1 *Reagents and conditions*: i, PMIDA, H_2O, 20 h; ii, TEOS, NH_4OH, EtOH (70%), 20 h; iii, APTMS, EtOH (70%), 20 h.

Table 1 EDX and elemental analysis data for the synthesized materials.

Nanocomposites	Elemental content (%)				Ratio of inorganic components Fe_3O_4/SiO_2 [c]	Content of organic components/mmol g^{-1}	
	Fe [a]	Si [a]	P [a]	C [b]		C_{APS} [d]	C_{PMIDA} [c]
MNPs–PMIDA	94.34	0	5.66	5.85	–	0	0.97
MNPs–SiO_2-1	77.12	22.88	0	0	69 : 31	0	0
MNPs–SiO_2-2	71.32	24.87	3.80	1.72	65 : 35	0	0.63
MNPs–SiO_2–APS-1	74.65	25.35	0	3.49	66 : 34	0.48	0
MNPs–SiO_2–APS-2	68.82	29.69	1.49	4.31	60 : 40	0.66	0.26

[a] Determined by EDX analysis. [b] Determined by CHN elemental analysis. [c] Calculated from the EDX data. [d] Calculated from the CHN elemental analysis data.

PMIDA in MNPs–PMIDA is retained on the surface of nanocomposites after coating with SiO_2 and APS (see Table 1). The saturation magnetization (M_s) of the materials regularly decreases depending on the increase in the SiO_2 content [Figure 3(*b*)].

Based on the published data on the sorption of Dox, it can be concluded that the Dox loading capacity is higher in the case of higher ratios of nanoparticles to Dox,[5,17] as well as at pH 7.4, compared to lower pH values.[5] To assess the effect of PMIDA, APS or both on the efficiency of loading Dox on nanocomposites with a shell of SiO_2, Dox sorption was carried out on all four types of synthesized materials (see Scheme 1) at a ratio of nanoparticles to Dox equal to 1 : 1.15 in an aqueous solution with neutral pH. The dimensions of the materials obtained after Dox sorption changed insignificantly: an example TEM image of MNPs–SiO_2–APS–Dox-2 is shown in Figure 1(*c*). The hydrodynamic parameters of the synthesized nanocomposites are shown in Figure 4(*a*) and Table 2.

Based on the fact that the intensity of the band in the region of 1700–1350 cm^{-1} in the FTIR spectrum is increased, the degree of Dox immobilization is the highest for SiO_2-coated nanocomposites compared to APS-modified ones (see Figure 2). At the same time, for PMIDA-containing materials, the intensity of the bands is higher in comparison with analogs not containing PMIDA, which indicates a significant role of PMIDA in the sorption of Dox. Loading efficiency (LE) and loading capacity (LC) (see Table 2) were quantified by UV spectroscopy data and calculated using formulas (1) and (2):

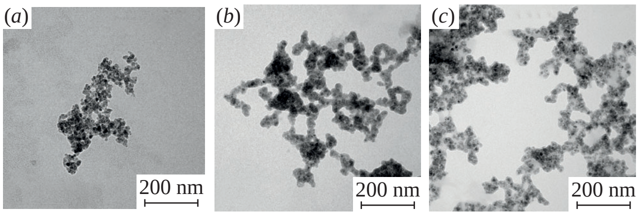

Figure 1 TEM images of SiO_2-modified nanocomposites (*a*) MNPs–SiO_2-1 and (*b*) MNPs–SiO_2-2 synthesized using bare and PMIDA-stabilized MNPs, respectively, as well as (*c*) MNPs–SiO_2–APS–Dox-2.

$$\mathrm{LE} = (m_{\mathrm{Dox\ load}} - m_{\mathrm{Dox}}) \times 100\% \,/\, m_{\mathrm{Dox\ load}}, \tag{1}$$

$$\mathrm{LC} = (m_{\mathrm{Dox\ load}} - m_{\mathrm{Dox}}) \times 100\% \,/\, m_{\mathrm{nanocomposite}}, \tag{2}$$

where $m_{\mathrm{Dox\ load}}$ is the weight (mg) of Dox loaded into the reaction, m_{Dox} is the weight (mg) of Dox in the supernatant and $m_{\mathrm{nanocomposite}}$ is the weight (mg) of the Dox-containing nanocomposite.

The best LC index of 25.7%, achieved for MNPs–SiO_2–2 nanoparticles, exceeds the loading capacity of a number of materials described in the literature, including those based on APS-modified ones,[12–17] and is comparable with the LC of 25.8% for mesoporous SiO_2 nanoparticles.[10]

Desorption of Dox was studied in phosphate buffer solutions with pH 5.8 and 7.4 by UV spectroscopy. The absorption spectra of Dox in the analyzed filtrates isolated after sorption and desorption coincide with the spectrum of the starting Dox, which indicates that its properties are retained during these procedures [Figure 4(*b*)]. All nanocomposites exhibit pH-dependent drug release [Figure 4(*d*)]. At the same time, desorption from MNPs–SiO_2–Dox-1 and MNPs–SiO_2–APS–Dox-1 proceeds much faster than from PMIDA-modified analogs. This can be explained by the presence of

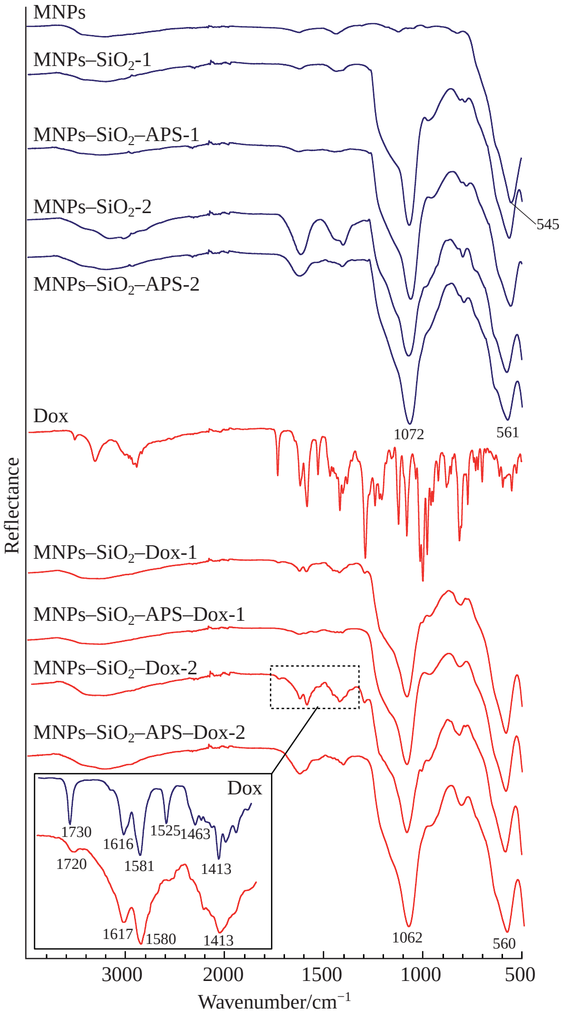

Figure 2 FTIR spectra of the synthesized nanocomposites (the inset shows an enlarged fragment of the IR spectrum in the region of 1800–1350 cm^{-1}).

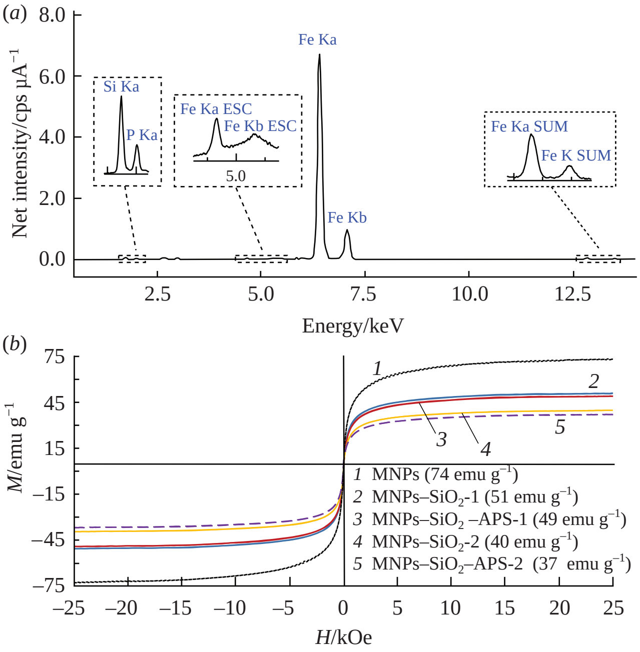

Figure 3 (*a*) EDX spectrum of MNPs–SiO$_2$-2. (*b*) Magnetization curves for the synthesized nanocomposites.

weaker bonds between Dox and the surface groups of these materials.

The formation of Dox complexes with small SiO$_2$ clusters[18] containing Si–OH groups, APS fragments and PMIDA molecules on the surface was studied by the DFT method in the gas phase using the ORCA 4.0.1 program (see Table 2).[19] It was shown that the complex of SiO$_2$–PMIDA with Dox has the best binding energy (Figure 5). In contrast, the SiO$_2$–APS complexes had lower modulus values (see Table 2 and Tables S1 and S2 in Online Supplementary Materials). DFT calculations suggest that the binding of SiO$_2$–PMIDA with Dox into a complex occurs as a result of the coordination of the PMIDA molecule on the SiO$_2$ surface due to the formation of the Si–O–P bond, as well as the formation of a hydrogen bond between the hydroxyl of the phosphonic group and the hydroxyl at the C(8) atom of Dox. In addition, the Dox molecule is coordinated by silanol groups on the cluster surface (see Figure 5). It has been shown that the values of the loading capacity of nanocomposites correlate with the binding energies of Dox complexes with functionalized SiO$_2$ clusters (see Table 2).

Thus, we obtained new nanocomposites with high loading capacity of Dox (up to 25.7%). A more efficient binding of Dox to the negatively charged surface of SiO$_2$ particles was shown compared to APS-modified ones containing positively charged amino groups. In the case of MNPs–SiO$_2$-2 and MNPs–SiO$_2$–APS-2 nanocomposites, the presence of PMIDA molecules on the surface significantly increases the sorption level in comparison with materials obtained without PMIDA. Based on DTF calculations, a mechanism for Dox binding to the surface of the synthesized nanocomposites was proposed. The resulting materials demonstrate the pH-dependent release of Dox. We believe that these nanocomposites could be used in the future to develop stimuli-responsive materials for targeted cancer chemotherapy.

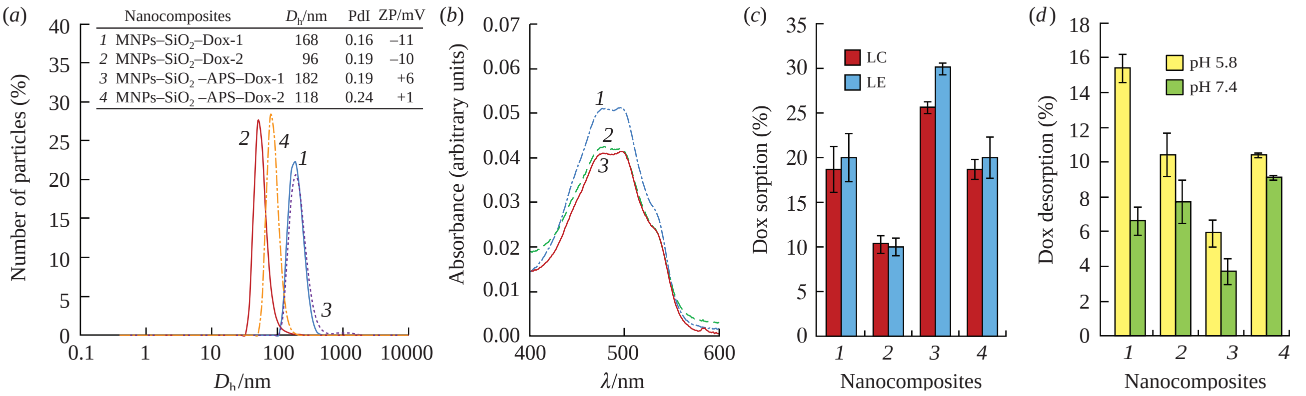

	Nanocomposites	D_h/nm	PdI	ZP/mV
1	MNPs–SiO$_2$–Dox-1	168	0.16	–11
2	MNPs–SiO$_2$–Dox-2	96	0.19	–10
3	MNPs–SiO$_2$–APS–Dox-1	182	0.19	+6
4	MNPs–SiO$_2$–APS–Dox-2	118	0.24	+1

Figure 4 (*a*) Dynamic light scattering (DLS) data for synthesized materials. (*b*) Absorption spectra of (*1*) the starting Dox solution, (*2*) filtrates after its sorption and (*3*) desorption from nanocomposites. (*c*) Efficiency of Dox sorption on synthesized nanocomposites: (*1*) MNPs–SiO$_2$-1, (*2*) MNPs–SiO$_2$–APS-1, (*3*) MNPs–SiO$_2$-2 and (*4*) MNPs–SiO$_2$–APS-2, and (*d*) subsequent release (the histogram shows wt% Dox relative to the amount of Dox loaded on the nanoparticles).

Table 2 Hydrodynamic parameters and loading capacity of the synthesized nanocomposites, as well as calculated binding energies for the Dox complexes with SiO_2 clusters containing various surface functional groups.

Nanocomposites	Functional groups on the nanocomposite surface	DLS data			LC (%)	$E_b{}^a$/kJ mol^{-1}
		D_h/nm	PdI	ZP/mV		
MNPs–SiO_2-1	Si–OH	168	0.16	–11	18.7 ± 2.6	–163.6
MNPs–SiO_2–APS-1	Si–OH, –NH_2	182	0.19	+6	10.3 ± 1.0	–37.6
MNPs–SiO_2-2	Si–OH, –PO_3H_2, –COOH	96	0.19	–10	25.6 ± 0.7	–318.20
MNPs–SiO_2–APS-2	Si–OH, –NH_2, –PO_3H_2, –COOH	118	0.24	+1	18.7 ± 1.1	

[a] The E_b values were calculated by the DFT method for the most optimized Dox complexes with SiO_2 clusters containing various functional groups that simulate the surface of the synthesized MNPs.

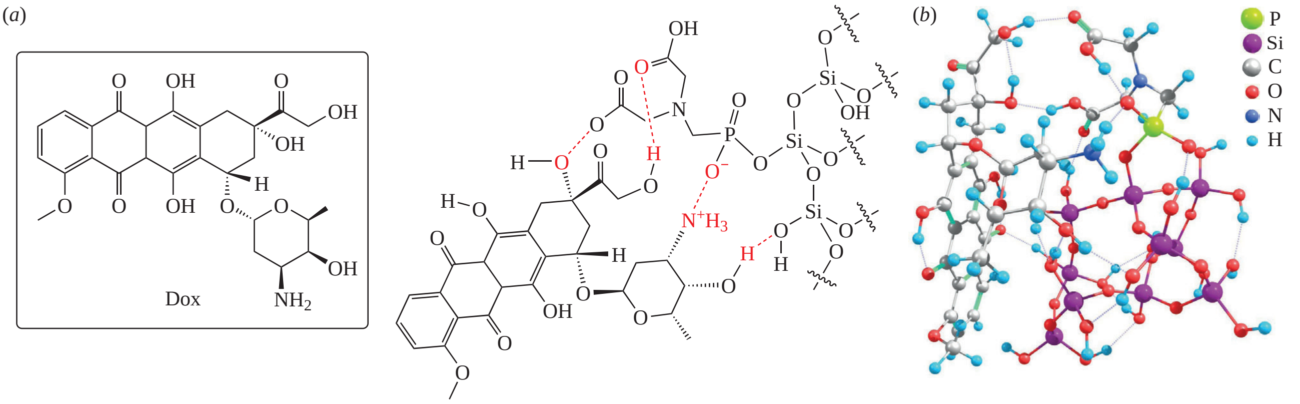

Figure 5 (*a*) Structural formula of doxorubicin (Dox) and the scheme of its binding to the surface groups of the MNPs–SiO_2-2 nanocomposite. (*b*) Complex of SiO_2–PMIDA cluster with Dox in water, which demonstrated the lowest binding energy (E_b) in DFT calculations.

This work was carried out with financial support from the Ministry of Science and Higher Education of the Russian Federation (grant no. 075-15-2020-777) using the equipment of the Center for Joint Use 'Spectroscopy and Analysis of Organic Compounds' at the I. Ya. Postovsky Institute of Organic Synthesis, Ural Branch of the Russian Academy of Sciences. Quantum chemical calculations were performed using the computing resources of the Center for Joint Use 'Supercomputer Center' of the N. N. Krasovskii Institute of Mathematics and Mechanics, Ural Branch of the Russian Academy of Sciences.

Online Supplementary Materials

Supplementary data associated with this article can be found in the online version at doi: 10.1016/j.mencom.2023.02.004.

References

1 M. Moros, J. Idiago-López, L. Asín, E. Moreno-Antolín, L. Beola, V. Grazú, R. M. Fratila, L. Gutiérrez and J. M. de la Fuente, *Adv. Drug Delivery Rev.*, 2019, **138**, 326.

2 H. Li, S. Yang, D. Hui and R. Hong, *Nanotechnol. Rev.*, 2020, **9**, 1265.

3 A. M. Demin, A. G. Pershina, A. S. Minin, O. Ya. Brikunova, A. M. Murzakaev, N. A. Perekucha, A. V. Romashchenko, O. B. Shevelev, M. A. Uimin, I. V. Byzov, D. Malkeyeva, E. Kiseleva, L. V. Efimova, S. V. Vtorushin, L. M. Ogorodova and V. P. Krasnov, *ACS Appl. Mater. Interfaces*, 2021, **13**, 36800.

4 Z. Dai, W. Wen, Z. Guo, X.-Z. Song, K. Zheng, X. Xu, X. Qi and Z. Tan, *Colloids Surf., B*, 2020, **195**, 111274.

5 A. M. Demin, A. V. Mekhaev, O. F. Kandarakov, V. I. Popenko, O. G. Leonova, A. M. Murzakaev, D. K. Kuznetsov, M. A. Uimin, A. S. Minin, V. Ya. Shur, A. V. Belyavsky and V. P. Krasnov, *Colloids Surf., B*, 2020, **190**, 110879.

6 M. V. Savvateeva, A. M. Demin, V. P. Krasnov and A. V. Belyavsky, *Anal. Biochem.*, 2016, **509**, 146.

7 N. C. Candian Lobato, A. de Mello Ferreira, P. G. Weidler, M. Franzreb, G. Cordeiro Silva and M. Borges Mansur, *Appl. Surf. Sci.*, 2020, **505**, 144565.

8 A. M. Demin, A. I. Maksimovskikh, A. V. Mekhaev, D. K. Kuznetsov, A. S. Minin, A. G. Pershina, M. A. Uimin, V. Ya. Shur and V. P. Krasnov, *Ceram. Int.*, 2021, **47**, 23078.

9 W. Sheng, W. Wei, J. Li, X. Qi, G. Zuo, Q. Chen, X. Pan and W. Dong, *Appl. Surf. Sci.*, 2016, **387**, 1116.

10 Y. Zhang, M. Dang, Y. Tian, Y. Zhu, W. Liu, W. Tian, Y. Su, Q. Ni, C. Xu, N. Lu, J. Tao, Y. Li, S. Zhao, Y. Zhao, Z. Yang, L. Sun, Z. Teng and G. Lu, *ACS Appl. Mater. Interfaces*, 2017, **9**, 30543.

11 Z. G. Denieva, U. A. Budanova and Yu. L. Sebyakin, *Mendeleev Commun.*, 2019, **29**, 32.

12 Y. Zhu and C. Tao, *RSC Adv.*, 2015, **5**, 22365.

13 S. Javanbakht, M. Shadi, R. Mohammadian, A. Shaabani, M. Ghorbani, G. Rabiee and M. M. Amini, *Mater. Chem. Phys.*, 2020, **247**, 122857.

14 T. N. Tram Nguyen, N. T. Trang Le, N. H. Nguyen, B. T. Kim Ly, T. D. Nguyen and D. H. Nguyen, *Microporous Mesoporous Mater.*, 2020, **309**, 110543.

15 S. Sadighian, K. Rostamizadeh, H. Hosseini-Monfared and M. Hamidi, *Colloids Surf., B*, 2014, **117**, 406.

16 A. M. Demin, A. V. Vakhrushev, M. S. Valova, A. S. Minin, D. K. Kuznetsov, M. A. Uimin, V. Ya. Shur, V. P. Krasnov and V. N. Charushin, *Russ. Chem. Bull.*, 2021, **70**, 987.

17 L.-L. Hu, J. Meng, D.-D. Zhang, M.-L. Chen, Y. Shu and J.-H. Wang, *Talanta*, 2018, **177**, 203.

18 M. Najafi, A. Morsali and M. R. Bozorgmehr, *Struct. Chem.*, 2019, **30**, 715.

19 F. Neese, *Wiley Interdiscip. Rev.: Comput. Mol. Sci.*, 2012, **2**, 73.

Received: 11th August 2022; Com. 22/6979